



## Phase inversion method for the preparation of Pebax® 3533 thin film membranes for CO<sub>2</sub>/N<sub>2</sub> separation

Lidia Martínez-Izquierdo<sup>a,b</sup>, Magdalena Malankowska<sup>a,b</sup>, Carlos Téllez<sup>a,b</sup>, Joaquín Coronas<sup>a,b,\*</sup>

<sup>a</sup> Instituto de Nanociencia y Materiales de Aragón (INMA), Universidad de Zaragoza-CSIC, 50018 Zaragoza, Spain

<sup>b</sup> Chemical and Environmental Engineering Department, Universidad de Zaragoza, 50018 Zaragoza, Spain

### ARTICLE INFO

Editor: Yunho Lee

#### Keywords:

Gas separation  
Pebax®  
Phase inversion  
Carbon dioxide  
Thin film composite membrane

### ABSTRACT

Thin film composite membranes of poly(ether-block-amide) copolymer Pebax® 3533 were prepared for the first time on asymmetric polysulfone supports by a phase inversion method. The casting solution concentration and the number of layers were varied to study their influence on the selective layer thickness and the gas separation performance. The casting solution concentrations of polymer dissolved in the 1-propanol/1-butanol mixture were 0.25, 0.5, 1.0 and 1.5 wt%. These conditions produced membranes with selective skin layers with thicknesses from 0.2 to 1.8 μm. All the membranes were characterized by scanning electron microscopy, thermogravimetric analysis and infrared spectroscopy. Furthermore, the intrinsic viscosity of all the casting solutions was studied to understand the effect of the polymer concentration on the homogeneity and the gas separation properties of the obtained membranes. In general, lower viscosity of casting solutions rendered to more defective skin layers, resulting in a higher number of layers required to obtain selective membranes. The gas separation performance was tested for the post-combustion 15/85 CO<sub>2</sub>/N<sub>2</sub> mixture at 25–50 °C and under a feed pressure of 3 bar. The best separation performance was achieved with the 0.5 wt% casting solution membranes after the deposition of four polymer layers, obtaining a CO<sub>2</sub> permeance of 127 GPU and a CO<sub>2</sub>/N<sub>2</sub> selectivity of 21.4 at 35 °C, the same selectivity of the corresponding dense membrane but with much higher permeance.

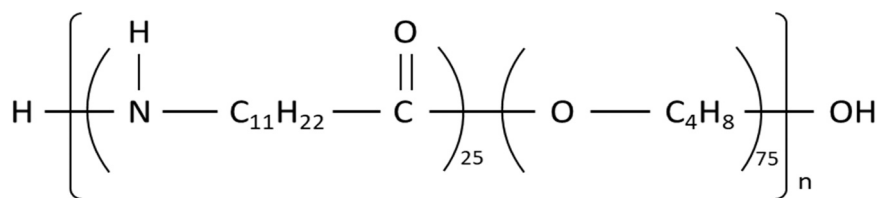
### 1. Introduction

Among the most common greenhouse gases, carbon dioxide (CO<sub>2</sub>) is considered to be the main cause of the global temperature rise. To alleviate this negative effect, there is a demand for CO<sub>2</sub> capture and sequestration technologies [1]. Such technologies must be able to remove CO<sub>2</sub> from fuels and exhaust gases to achieve a clean stream to be used in other industrial processes [2]. Within these processes, post-combustion CO<sub>2</sub> capture is the simplest approach to be implemented due to its ease to be adapted to the already existing industrial facilities. In this field, technologies like physical or chemical absorption with amines, cryogenic distillation, and adsorption [3] have been the most commonly used for CO<sub>2</sub> capture, although some drawbacks such as their potential toxicity or the difficulties derived from the regeneration of the solvent (in the case of chemical absorption with amines) resulted in many studies focusing on greener approaches [4]. With this aim, gas separation via polymeric membranes is now gaining more attention over the traditional techniques due to its well-known advantages, i.e. mechanical simplicity, easy to scale up, lower energy consumption and

cost, and smaller footprint [5].

CO<sub>2</sub> capture from post-combustion streams is based on the separation of CO<sub>2</sub> from a CO<sub>2</sub>/N<sub>2</sub> mixture, where CO<sub>2</sub> concentration can go from ca. 15% in case of typical combustion processes to ca. 30% in case of stainless steel and cement industries, important producers of this gas. In this sense, working with polymers with excellent properties and facilitated transport parameters for this mixture is mandatory to obtain effective membranes. Poly(ether-block-amide) copolymers (PEBA, usually commercialized as Pebax®) are composed of two different polymer segments (polyamide (PA) and polyether (PE)). Each segment provides different material characteristics and combined make Pebax® a very promising candidate [6–11]. In this work, Pebax® 3533 code was used due to its solubility in an alcohol (1-propanol/1-butanol) mixture, which suggests higher chemical stability of the obtained membranes when exposed to moisture since the most common Pebax® 1657 membranes are obtained from water/ethanol polymer solutions. A good stability of membranes to water vapor is needed since in real post-combustion processes coal-derived flue gases not only contain CO<sub>2</sub> and N<sub>2</sub> but also oxygen, SO<sub>x</sub> and NO<sub>x</sub> compounds and other minor contaminants like

\* Corresponding author at: Instituto de Nanociencia y Materiales de Aragón (INMA), Universidad de Zaragoza-CSIC, 50018 Zaragoza, Spain.  
E-mail address: [coronas@unizar.es](mailto:coronas@unizar.es) (J. Coronas).



Scheme 1. Pebax® 3533 chemical structure.

water vapor [12].

To achieve an efficient separation, which exceeds the Robeson trade-off relationship between permeability and selectivity [13], an ideal membrane for gas separation should be as thin as possible, to maximize the flux through it (high CO<sub>2</sub> permeance), highly selective and mechanically robust [14]. To accomplish this target, composite membranes must be prepared with a very thin selective layer.

In the open literature, the methods for preparing composite membranes are diverse. The most typical approaches include dip-coating [15, 16], spin-coating [17,18] and interfacial polymerization [19], being the dip-coating the most commonly used for gas separation membranes due to its easy implementation. According to this method, Ren et al. prepared a multilayer polyetherimide (PEI)/polydimethylsiloxane (PDMS)/Pebax® 1657/PDMS composite membrane [11]. With this composite membrane the authors achieved, at 5 bar and 25 °C, a CO<sub>2</sub> permeance of 157 GPU and a CO<sub>2</sub>/N<sub>2</sub> selectivity of 64. Zhao et al. developed a similar multilayer structure based on a polysulfone (PSF) support covered by a PDMS gutter layer modified with plasma and a Pebax® 1657 selective layer [20]. In this case, the authors obtained a CO<sub>2</sub> permeance of 170 GPU and an ideal CO<sub>2</sub>/N<sub>2</sub> selectivity of 49, measured at 7 bar and 30 °C.

In this work, we report the preparation for the first time of Pebax® 3533 thin film composite membranes via a phase inversion method (immersion-precipitation with a non-solvent). Following this approach, different membranes were prepared varying the concentration of Pebax® 3533 in the casting solution (0.25, 0.5, 1.0 and 1.5 wt%) as well as the number of layers deposited (1–6). The best condition found was chosen to prepare supported membranes by dip-coating, tested for the separation of CO<sub>2</sub>/N<sub>2</sub> mixtures. Finally, Pebax® 3533 has only rarely been studied, and in a few publications: as dense membrane for CO<sub>2</sub> separation [21], to improve impact strength [22] and in drug release [23].

## 2. Experimental

### 2.1. Materials

Polysulfone (Udel® P-3500 LCD) was purchased from Solvay Advanced Polymers. Polyether-block-amide, Pebax® 3533 SA 01 MED (Scheme 1) (comprising 75 wt% poly (tetramethylene oxide) (PTMO) and 25 wt% aliphatic polyamide (PA12)) in the form of pellets was kindly provided by Arkema, France. The solvents, N-methyl-2-pyrrolidone (NMP), 1-propanol and 1-butanol were purchased from Panreac, Labbox and Scharlab, Spain, respectively. All gases used for the separation tests were of research grade (greater than 99.995% of purity) and supplied by Abelló Linde S.A., Spain. All gases, polymers and solvents were used as received.

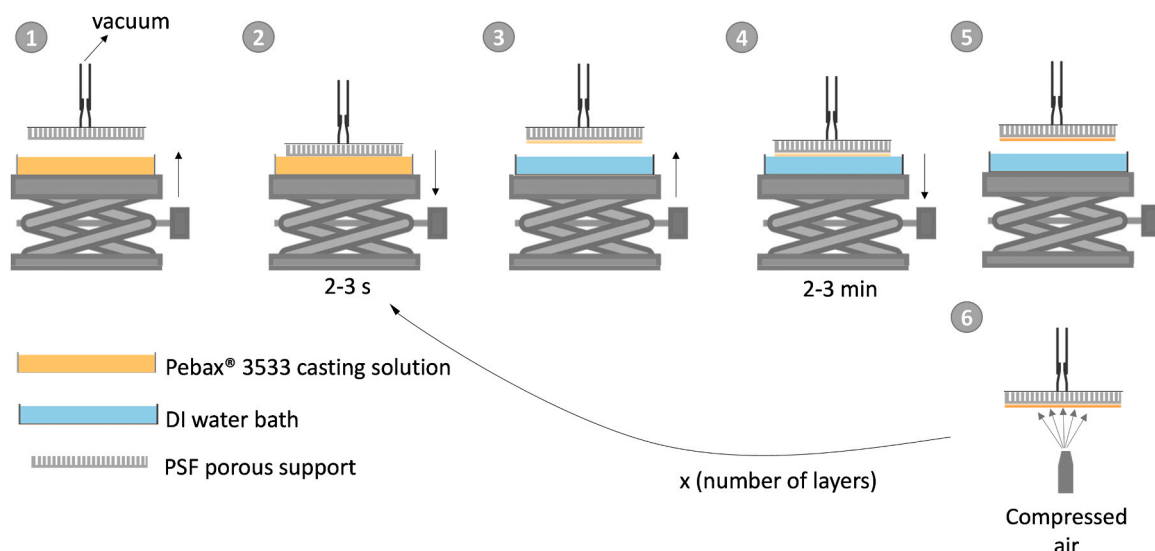
### 2.2. Methods

#### 2.2.1. Preparation of Pebax® 3533 self-supported dense membranes

To compare with the supported membranes and confirm the applicability of the method, self-supported dense membranes were prepared by casting followed by solvent evaporation. Pellets of Pebax® 3533 were first dissolved in a mixture 3:1 (v/v) of 1-propanol:1-butanol, stirred under reflux at 80 °C for 2 h to obtain a 3 wt% casting solution. Once cooled down to room temperature, this solution was cast onto a glass Petri dish and left for solvent evaporation and drying overnight at room temperature in a solvent saturated atmosphere [5]. Finally, the membranes were peeled off from the Petri dishes and treated in an oven at 40 °C for 48 h for the complete removal of the solvent. The thickness of the membranes prepared in this way was approximately 55 µm.

#### 2.2.2. Preparation of PSF asymmetric supports

The PSF supports were prepared by the phase inversion technique as follows [4]: a dope solution of 20 wt% was prepared dissolving PSF in



Scheme 2. Layer-by-layer method by phase inversion. Including drying time (ca. 1 min), the total time is 4–5 min.

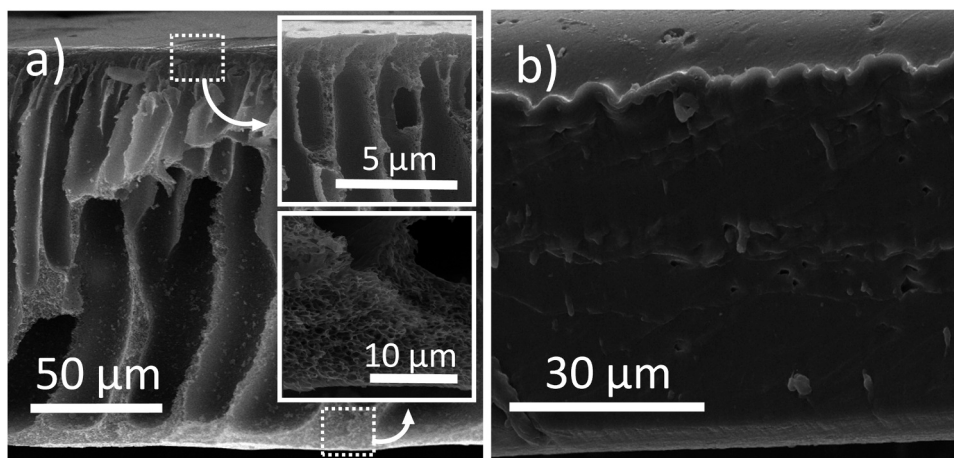


**Fig. 1.** Cross-section images of the PSF support (a) and the Pebax® 3533 dense membrane prepared by the conventional casting-solution method (b). Insets correspond to the top and bottom sides of the PSF support.

NMP under stirring at room temperature overnight. Once degassed, the polymer solution was cast onto a Teflon plate using an Elcometer 4340 Automatic Film Applicator at a thickness of 250  $\mu\text{m}$  and using a casting speed of 0.04  $\text{m s}^{-1}$ . Immediately after casting, the membranes were immersed in a water bath for 1 h at room temperature, where the phase inversion occurred. After complete precipitation, the membranes were transferred to a deionized (DI) water bath where they remained overnight and then they were rinsed with isopropanol. The PSF supports were finally dried at 100  $^{\circ}\text{C}$  for 24 h.

### 2.2.3. Preparation of Pebax® 3533 supported membranes by phase inversion and dip-coating

To prepare the thin film composite (TFC) supported membranes by phase inversion, the first step was to obtain the polymer solution by dissolving Pebax® 3533 in the mixture of 1-propanol:1-butanol (3:1 v/v) at different concentrations (0.25, 0.5, 1.0 and 1.5 wt%). These solutions were obtained following the steps previously explained for dense membranes. With these solutions, supported membranes were prepared applying different number of layers on top of PSF supports by phase inversion following the steps in Scheme 2. Firstly, PSF support was horizontally fixed with the aid of a vacuum pump. Pebax® 3533 casting solution, in the form of a liquid, was applied just to the selective side of the support. In the second step, the Pebax® solution, previously poured into a Petri dish, was put in contact with the support by lifting the platform where the casting solution was located and maintained in contact for approximately 2–3 s. Immediately after this short time, the platform was lowered again and the Petri dish containing the Pebax® solution was replaced by another one with DI water (third step). In the fourth and fifth steps, the same procedure was carried out, but this time with the DI water bath, where the phase inversion of Pebax® took place. After 2–3 min in contact with water, the membrane was gently dried for ca. 1 min with compressed air (sixth step). Once the excess of water was removed, the membrane was ready to repeat the cycle, as many times as necessary depending on the desired number of layers and membrane total thickness. The total time required to complete each cycle was scarcely 4–5 min. Finally, membranes were dried in an oven at 40  $^{\circ}\text{C}$  for 48 h before gas permeation tests. Membranes obtained by this method were abbreviated as Xwt%\_Y, where X is the concentration of Pebax® in the casting solution, and Y the number of layers.

The best conditions found with the supported membranes prepared by phase inversion were applied to obtain the conventional ones by dip-coating [15]. Briefly, a casting solution with a Pebax® concentration of 0.5 wt% was obtained as explained before. PSF supports were horizontally fixed with the aid of a vacuum pump. Once fixed, the Pebax® 3533 solution was dip-coated during 30 s. Membranes were then placed in an

oven at 40  $^{\circ}\text{C}$  to allow solvent evaporation for 1 h, before the deposition of the remaining layers. This procedure was repeated three more times to obtain a membrane with a total of 4 layers. Finally, membranes were dried in an oven at 40  $^{\circ}\text{C}$  for 48 h before characterization. Membranes prepared this way were called 0.5 wt%\_4\_dip-coating.

### 2.3. Membrane characterization

Scanning electron microscopy (SEM) images of the membranes were obtained using an Inspect F50 model scanning electron microscope (FEI), operated at 10 kV. This instrument was also used for measuring (at 5–6 different positions along the membrane) the thickness of the selective skin layer. Cross-sections of membranes were prepared by freeze-fracturing after immersion in liquid  $\text{N}_2$  and subsequently coated with Pd. Viscosity tests were conducted with a SMART L Fungilab Rotational viscometer. Casting solutions (~15 mL) placed in an APM/B adapter were subjected to different rotational speeds (from 75 to 200 rpm) at 24  $^{\circ}\text{C}$ . Fourier transform infrared spectroscopy (FTIR) was performed with a Bruker Vertex 70 FTIR spectrometer equipped with a DTGS detector and a Golden Gate diamond ATR accessory. The spectra were recorded by averaging 40 scans in the wavenumber range of 4000–600  $\text{cm}^{-1}$  at a resolution of 4  $\text{cm}^{-1}$ . Thermogravimetric analyses (TGA) and differential thermogravimetry (DTG) were carried out using a Mettler Toledo TGA/STDA 851e. Small pieces of membranes (~3 mg) placed in 70  $\mu\text{L}$  alumina pans were heated under an airflow (40  $\text{cm}^3(\text{STP}) \text{min}^{-1}$ ) from 35 to 700  $^{\circ}\text{C}$  at a heating rate of 10  $^{\circ}\text{C min}^{-1}$ .

### 2.4. Gas permeation tests

Membranes were cut and placed in a module consisting of two stainless steel pieces and a 316LSS macro-porous disk support (Mott Co.) with a 20  $\mu\text{m}$  nominal pore size. Membranes, 2.12  $\text{cm}^2$  in area, were gripped inside with Viton O-rings. To control the temperature of the experiment (in the 25–50  $^{\circ}\text{C}$  range), which has an effect on gas separation, the permeation module was placed in a UNE 200 Memmert oven. Although in real post-combustion systems the flue gas pressure is ambient, there are some factors that must be taken into account when choosing the separation conditions for efficient separation of  $\text{CO}_2$ . In 2010, Baker and co-workers [12] estimated the impact that some factors such as pressure generation (using compressors or vacuum pumps) and membrane relative area have on the total separation cost. In this study, they found that working at low pressures implies a rise in capture cost because of excessive membrane areas. Otherwise, working at very high pressures means an excessive energy charge. This information suggested that moderate pressures must be reached at the feed side to achieve

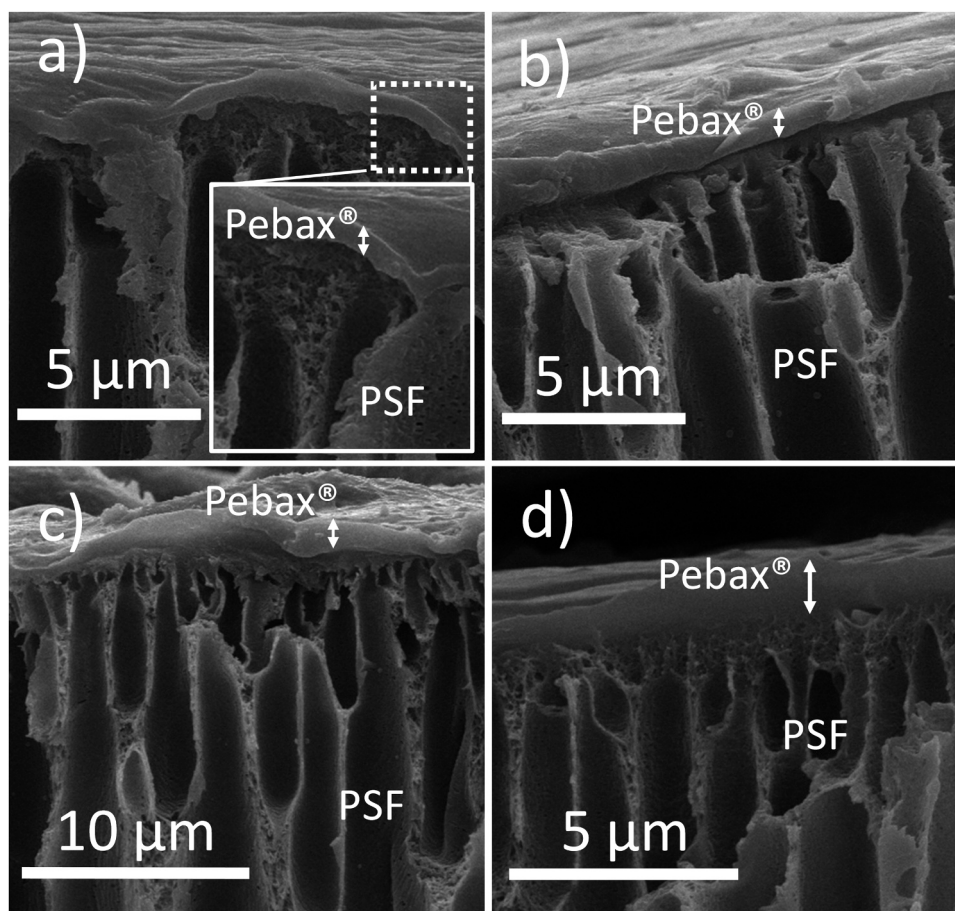


**Fig. 2.** Cross-section images of the supported membranes prepared with the 0.5 wt% casting solution via phase inversion after the deposition of 3 (a), 4 (b), 5 (c) and 6 (d) Pebax® layers. Inset in (a) corresponds to the top layer of the membrane.

competitive separations with a reduced final cost. For this reason, in this work, the gas separation measurements were carried out by feeding the post-combustion gaseous mixture of CO<sub>2</sub>/N<sub>2</sub> (15/85 cm<sup>3</sup>(STP) min<sup>-1</sup>) to the feed side at an operating pressure of 3 bar to favor CO<sub>2</sub> permeation. Gas flows were controlled by two mass-flow controllers (Alicat Scientific, MC-100CCM-D). The permeate side of the membrane was swept with a 4.5 cm<sup>3</sup>(STP) min<sup>-1</sup> of He, at atmospheric pressure (~1 bar) (Alicat Scientific, MC-5CCM-D). Concentrations of N<sub>2</sub> and CO<sub>2</sub> in the outgoing streams (permeate side) were analyzed online by an Agilent 3000 A micro-gas chromatograph. Permeances were calculated in GPU (gas permeance unit, 10<sup>-6</sup> cm<sup>3</sup>(STP) cm<sup>-2</sup> s<sup>-1</sup> cm Hg<sup>-1</sup>), once the steady state of the exit stream was reached (at least after 2 h). At this stage, membrane samples are considered to be fully dried. The separation selectivity was calculated as the ratio of permeances.

### 3. Results and discussion

#### 3.1. Membranes preparation and characterization

Fig. 1a and b show the cross-sections of the PSF support and the Pebax® 3533 dense membrane, respectively, prepared by the conventional casting solution method. These images were taken for comparison with the supported membranes. As can be seen in Fig. 1a, the PSF support prepared in this work has a thickness of around 150 μm and is constituted by two different porous layers, finger-like macropores at the top of the film and thick sponge-like micropores at the bottom. Moreover, Fig. 1b confirms the Pebax® 3533 dense morphology without the existence of apparent porosity, as expected for this kind of polymers when prepared by the casting-solution technique. Membranes prepared

**Table 1**  
Thickness of supported membranes prepared in this work via phase inversion.

Membrane	Pebax® 3533 (wt%)	Layers	Thickness (μm)	Thickness increase (μm)
1.5 wt%_1	1.5	1	1.0 ± 0.2	1.0
1.5 wt%_2	1.5	2	1.8 ± 0.1	0.8
1.0 wt%_1	1.0	1	0.5 ± 0.1	0.5
1.0 wt%_2	1.0	2	1.5 ± 0.1	1.0
0.5 wt%_3	0.5	3	0.4 ± 0.1	0.4
0.5 wt%_4	0.5	4	0.7 ± 0.2	0.3
0.5 wt%_5	0.5	5	1.0 ± 0.2	0.3
0.5 wt%_6	0.5	6	1.3 ± 0.3	0.3
0.25 wt%_4	0.25	4	0.2 ± 0.0	0.2
0.25 wt%_5	0.25	5	0.5 ± 0.0	0.3
0.25 wt%_6	0.25	6	0.8 ± 0.0	0.3

in this way had a thickness of approximately 55 μm.

Pebax® 3533 thin film composite membranes (TFC) were prepared by phase inversion method on top of asymmetric PSF supports. Although this approach has been widely used for the preparation of asymmetric supports [24], to the best of our knowledge, only a recent article published in our research group considers this route for Pebax®-type polymers (Pebax® 1041) [4]. In contrast to this previous work, in which a polymer emulsion was drop-cast on a porous support, here we focus on the preparation of thin film composites of Pebax® 3533/polysulfone (PSF) via layer-by-layer method. An ideal membrane for gas separation must be as thin as possible to reach a high flow through it without losing



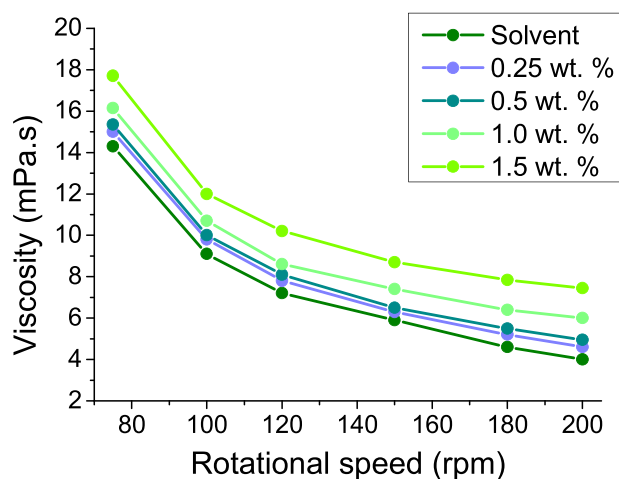


Fig. 3. Viscosity tests conducted at 24 °C and different rotational speeds for all the casting solution concentrations tested (0.25, 0.5, 1.0 and 1.5 wt%).

selectivity. To this aim, different conditions were tested in this work varying the concentration of Pebax® in the casting solution as well as the number of layers applied on top of the supports. Fig. 2a–d show the supported membranes prepared with the 0.5 wt% casting solution after the application of 3, 4, 5 and 6 polymer layers, respectively. TFC membranes prepared with the casting solutions of 0.25, 1.0 and 1.5 wt% are shown in Figs. S1–S3 of the SI, respectively. It can be seen that in all cases a very thin layer of Pebax® was deposited on top of the PSF supports (ranging from 400 nm to 1.3 μm, see Table 1) and that the number of layers cannot be differentiated. Furthermore, dense morphology obtained in all cases differs from the high-porosity expected in membranes prepared via phase inversion. Since Pebax®-type polymers behave as an elastomer-thermoplastic, such differences in morphology could be related to the collapse of the porous structure during the drying state. This behavior was also found by Sánchez-Laínez et al. in Pebax® 1041 membranes when prepared through the phase inversion method [4].

The thickness of each supported membrane obtained by SEM is collected in Table 1. As expected, for the same number of layers, the selective layer total thickness decreased when the casting solution concentration was lower. Besides, for the same casting solution concentration, the total thickness increased with the number of layers. Table 1 also shows the contribution of each layer to the thickness increase. In the case of the membranes prepared with the 0.5 wt% casting solution, for example, each additional layer made the total thickness to increase by ca. 300 nm. With this in mind, a total thickness of 900 nm would be expected for the 3-layered membrane instead of 400 nm. This difference could be due to the slight pore filling with the casting solution and the compatibility of the Pebax® polymer with the support. Once the support is covered with a layer of Pebax®, regardless of the thickness, compatibility increases and so does the homogeneity of the deposited Pebax® layers. The penetration of the casting solution into the support porosity is favored with less concentrated and less viscous polymer solutions.

From these results, we can conclude that from casting solution concentrations of 1.0 wt%, the more diluted the casting solution is, the more pore filling takes place and more defects must be repaired by the subsequent coatings. Therefore, a greater number of Pebax® layers will be required to obtain a homogeneous supported membrane. This statement can be justified if we take into account the casting solution viscosities. Fig. 3 shows the intrinsic viscosity of each casting solution concentration tested in this work at different rotational speeds compared with that of the pure mixture of solvents. As expected, the most concentrated casting solutions resulted in the most viscous ones as well. Such differences in viscosity seem to have an impact on the final characteristics of the Pebax® skin layer, as reduced solution viscosity is usually translated

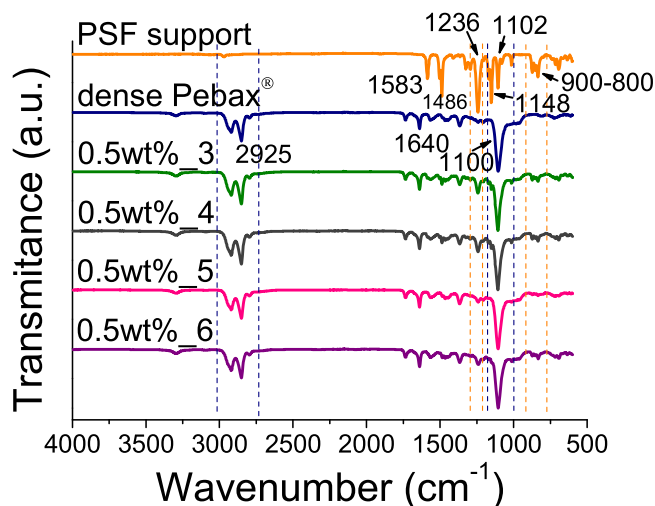


Fig. 4. FTIR-ATR spectra of membranes prepared by phase inversion with the 0.5 wt% casting solution concentration and a different number of layers (from 3 to 6) compared to that of the bare PSF support and the Pebax® 3533 dense membrane.

into faster exchange rate between casting solution solvent and water during the phase inversion. This phenomenon may lead to the formation of macro-voids (defects) [25]. Furthermore, for all cases, the viscosity decreased with the rotational speed, which means that all solutions behave as non-Newtonian pseudo-plastic fluids.

The chemical structures of the TFC membranes were also studied using an FTIR-ATR spectrometer. Fig. 4 shows the FTIR spectra of the supported membranes prepared with the 0.5 wt% casting solution, compared to that of the bare PSF support and the self-supported Pebax® 3533 dense membrane. The same comparison can be found in Fig. S4 of the SI, corresponding to the membranes prepared with the rest of the casting solutions tested (0.25, 1.0 and 1.5 wt%). As seen in these figures, several bands can be differentiated in the PSF spectrum. Bands at 1583 and 1486  $\text{cm}^{-1}$  are associated to the aromatic  $\text{C}=\text{C}$  stretching vibration [26]. The strong band that appears at 1236  $\text{cm}^{-1}$  is related to the asymmetric  $\text{C}-\text{O}-\text{C}$  stretching of the aryl ether. Symmetric and asymmetric  $\text{O}=\text{S}=\text{O}$  stretching of the sulfone group is visible in the bands at 1148 and 1102  $\text{cm}^{-1}$ . Finally, the two bands in the range of 900–800  $\text{cm}^{-1}$  correspond to the vibrations of the aliphatic  $\text{C}-\text{H}$  bonds [27]. In the case of the Pebax® 3533 spectrum, three main bands can be differentiated at 2925, 1640 and 1100  $\text{cm}^{-1}$  associated to both, the polyamide and the PTMO segments. Regarding the hard segment (PA-12), the band at 1640  $\text{cm}^{-1}$  corresponds to the vibrations of the  $\text{H}-\text{N}-\text{C}=\text{O}$  group [28]. Vibrations corresponding to the soft segment (PTMO) are visible in the bands at 2925 and 1100  $\text{cm}^{-1}$ , assigned to the stretching and bending vibrations of the aliphatic  $\text{C}-\text{H}$  group and the stretching vibration of the  $\text{C}-\text{O}-\text{C}$  ether group, respectively, which are in accordance with the literature [4,29]. Some of these main bands can be appreciated in the TFC spectrum. Fig. S4a shows the spectra of the TFC membranes prepared with the 1.5 wt% casting solution, which confirms that just with a single layer of Pebax® the surface of the porous support was covered uniformly since no band associated to the PSF can be appreciated. In contrast, when decreasing the casting solution concentration, for the TFC membranes prepared with the 1.0 wt% casting solution (Fig. S4b), the bands at 1236  $\text{cm}^{-1}$  and 900–800  $\text{cm}^{-1}$ , associated to the  $\text{C}-\text{O}-\text{C}$  stretching and  $\text{C}-\text{H}$  bonds of the PSF, are visible. In spite of that, the bands related to the Pebax® selective layer are stronger, indicating that bands of PSF observed can be due to the Pebax® thickness, which is thinner than that obtained with the more concentrated solution. These bands disappear when applying a second polymer layer. The same behavior is observed for the membranes prepared with the 0.5 wt% casting solution (Fig. 4). However, the strong bands at 1236

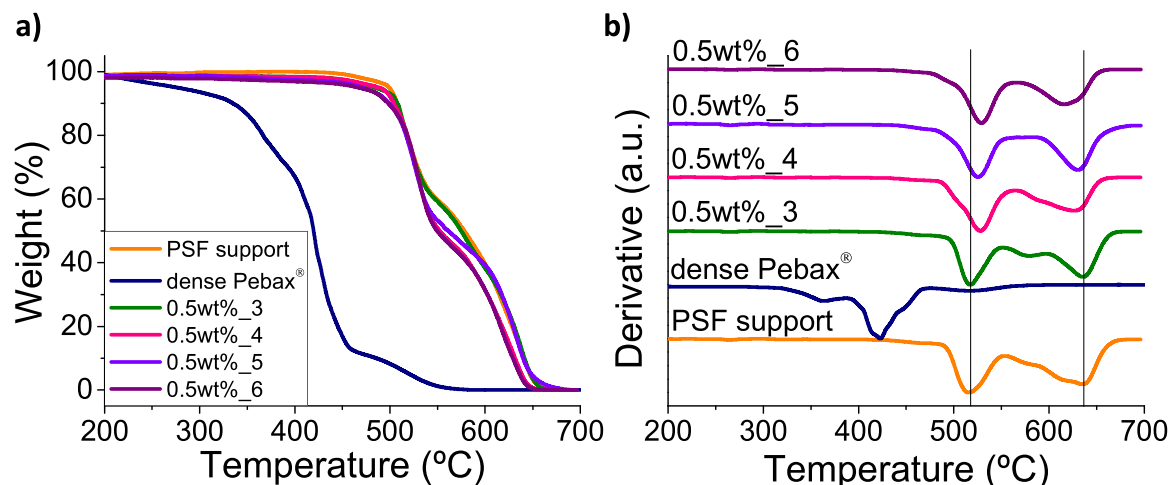


Fig. 5. TGA and DTG analyses of TFC membranes prepared by the phase inversion method with the 0.5 wt% casting solution compared to that of the PSF support and the bare Pebax® 3533.

and 900–800  $\text{cm}^{-1}$  are present in all cases, no matter the number of layers applied. In the case of membranes prepared with more diluted casting solution (Fig. S4c), the spectra obtained with all samples are more similar to that of the PSF support, despite the fact that the thicknesses of membranes prepared with 0.25 wt% casting solution after 5 and 6 layers are analogous to those of the membranes prepared with the 0.5 wt% solution after 4 and 5 layers, respectively. Such differences could be due to some defects possibly related to the concentration of the casting solution, which alters the viscosity and hence the behavior of the polymer in the phase inversion process [30–32]. This statement was confirmed when testing the membranes for the  $\text{CO}_2/\text{N}_2$  gas separation (see gas permeation section). Furthermore, an additional comparison illustrating the differences between each casting solution concentration is shown in Fig. S5 of the SI. In this figure, the FTIR spectra of the supported membranes prepared with each casting solution concentration after the deposition of 1 layer are compared with that of the bare PSF and the Pebax® 3533 dense membrane. As can be seen, this figure also demonstrates the previous statement. As the casting solution concentration decreases, the bands associated to the PSF support are stronger whereas that associated to the Pebax® becomes weaker. This fact confirms the need to apply more layers to the PSF when a very diluted solution is used.

The thermal stability of the membranes was studied by thermogravimetric analysis. The TGA and DTG results of the supported membranes prepared with the 0.5 wt% casting solution, compared with that of the bare PSF and Pebax® 3533 can be visualized in Fig. 5. As expected, due to the ultrathin layers deposited on top of the PSF supports, the thermal stability of membranes remains almost the same. In fact, Pebax® maximum degradation peak at 422 °C cannot be appreciated in TFC thermograms. Otherwise, only the peaks related to the thermal degradation of PSF at 515 and 635 °C are visible in the supported membranes, despite containing two different polymers. The greater proportion of PSF is responsible for this behavior [33]. Apart from that, TGA curves of the membranes prepared with 4–6 layers of Pebax® show a greater weight loss in the first degradation step, which suggest that the thermal degradation of the Pebax® selective layer is taking place at the same time as the PSF support. Furthermore, while degradation peaks of the membrane prepared with the lowest number of layers (0.5 wt%<sub>3</sub>) remained unaltered, it can be seen that the maximum PSF degradation that takes place at 515 °C was delayed in membranes with 4, 5 and 6 layers. Such delay can be related to a diffusion limitation, as PSF pores are covered by the more restrictive to the gas passage Pebax® 3533 selective layer. The same behavior was found for the rest of the casting solution concentrations tested in this work, whose thermograms can be

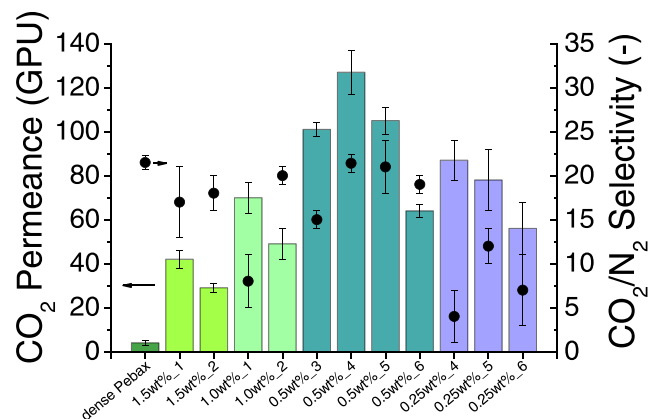


Fig. 6. Comparison of the  $\text{CO}_2$  permeance and  $\text{CO}_2/\text{N}_2$  selectivity of membranes prepared via phase inversion obtained at 35 °C and 3 bar. Bars stand for permeance and scatters for selectivity.

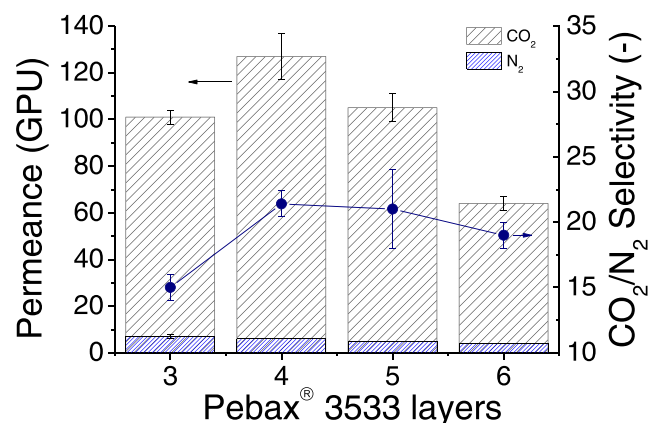


Fig. 7. Comparison of the gas separation results obtained for the supported membranes prepared with the 0.5 wt% casting solution tested at 35 °C and a feed pressure of 3 bar.

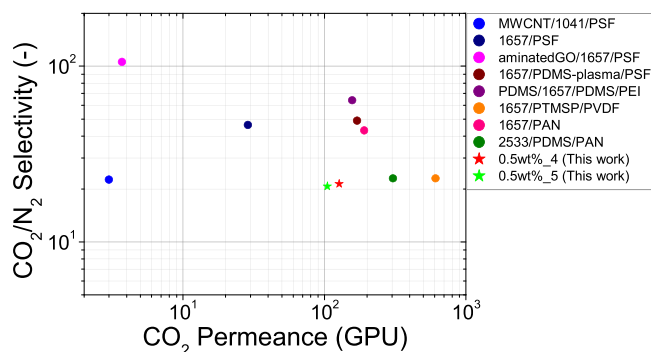


Fig. 8. Comparison of the separation performance of Pebax® based supported membranes. Conditions used for each membrane are specified in Table S2.

found in Figs. S6–S8 of the SI.

### 3.2. Gas permeation tests

The gas separation performance of the supported membranes was tested for the CO<sub>2</sub>/N<sub>2</sub> mixture under a feed pressure of 3 bar and 35 °C and can be seen in Fig. 6. In this figure, error bars correspond to the testing of at least three different membrane samples at the same conditions. Data shown in this figure are also collected in Table S1 of the SI. As expected, CO<sub>2</sub> permeance increased with the dilution of the Pebax® solution and decreased with the application of additional layers. However, some deviations were found for the membranes prepared with the most diluted solutions. In the case of those prepared with the 0.5 wt% casting solution, far from expected, the CO<sub>2</sub> permeance of the membrane with three polymer layers was lower than that with four and even five layers, these permeances being 101 ± 3 GPU, 127 ± 10 GPU and 105 ± 6 GPU, respectively. As shown in Fig. 7, such deviation could be related to the higher N<sub>2</sub> permeance of membranes prepared with three layers. In fact, N<sub>2</sub> permeance decrease with the application of additional layers. This phenomenon suggests the presence of micro-defects at the top layer of the 0.5 wt%<sub>3</sub> membranes, which hinder the selective diffusion of CO<sub>2</sub> molecules with the consequential decrease of selectivity. These defects were repaired after the application of an additional layer, which acts as healing and increased not only the CO<sub>2</sub> permeance but also the membrane selectivity. After the application of four Pebax® 3533 layers, the supported membranes followed the typical behavior described before. Otherwise, the lower CO<sub>2</sub> permeances of the membranes prepared with the 0.25 wt% casting solution compared to that of the 0.5 wt%, could be due to the decrease in the solution viscosity. As mentioned before, the reduction in viscosity can favor the pore penetration hindering the diffusion of gas molecules. Apart from that, defects obtained with this casting solution were more visible, since it was not possible to obtain a membrane with a CO<sub>2</sub>/N<sub>2</sub> selectivity similar to that of the dense Pebax® 3533, ca. 21.5. In addition, larger error bars demonstrate a worse reproducibility. With this data, the optimal casting solution corresponds to that prepared with the 0.5 wt% of Pebax® and the best results were achieved with the application of four and five layers on top of the PSF supports. For these membranes, the CO<sub>2</sub>/N<sub>2</sub> selectivity was the same as that of the dense Pebax® 3533. To further validate this procedure, supported membranes were also prepared by the conventional dip-coating method. Gas separation results (Fig. S9), indicated that the CO<sub>2</sub> permeance of the membranes prepared by dip-coating was lower (61 ± 15 GPU) than that of those prepared by phase inversion (127 ± 10 GPU), whereas the selectivity was almost unaltered. These results suggest that a greater pore filling takes place when using the conventional dip-coating method, since the time needed to evaporate the solvent allows the casting solution to penetrate into the support pores. In the case of membranes prepared by phase inversion this phenomenon is reduced due to the very fast precipitation of the

Table 2

Apparent activation energies of Pebax®-type films reported in the literature.

Polymer	E <sub>p</sub> CO <sub>2</sub> (kJ mol <sup>-1</sup> )	E <sub>p</sub> N <sub>2</sub> (kJ mol <sup>-1</sup> )	Reference
Pebax® 1657	13.3	30.4	[39]
Pebax® 1657	14.9	28.0	[5]
Pebax® 1657	18.6	32.0	[40]
Pebax® 2533	16.7	27.2	[40]
Pebax® 2533	18.2	31.0	[41]
Pebax® 1074	13.4	30.3	[37]
Pebax® 3533	14.2	29.6	This work

polymer. Therefore, it can be concluded that the membrane preparation method developed in this work can be used in the same way as the conventional methods to achieve perm-selective membranes, with the advantages of being an easier and faster procedure, requiring each layer just 4–5 min to be completely formed, and being able to enhance the performance of membranes increasing the CO<sub>2</sub> permeance. It is worth mentioning that a certain number of Pebax® coatings is needed to conform supported membranes with desirable separation properties. This is because the first coatings act as a gutter layer for the subsequent polymer layers. However, a clear trade-off is established as a high number of layers punish the CO<sub>2</sub> permeance without improving the CO<sub>2</sub>/N<sub>2</sub> separation selectivity.

An additional comparison with other Pebax® based supported membranes can also be found in Fig. 8 and Table S2. Fig. 8 shows a CO<sub>2</sub>/N<sub>2</sub> log-log plot similar to that used by Robeson to compare the performance of different membranes [13]. In this case, the best supported membranes prepared in this work (0.5 wt%<sub>4</sub> and 0.5 wt%<sub>5</sub>) are plotted together with other Pebax® based membranes reported in bibliography [4,11,20,34–36]. As seen in Fig. 8, both the 0.5 wt%<sub>4</sub> and 0.5 wt%<sub>5</sub> supported membranes demonstrate exceptional gas separation performances, being also close to those previously reported for this kind of polymers. It is worth mentioning that this Pebax® code has not been as widely studied as other codes such as Pebax® 1657, and never as a thin composite membrane. In consequence, this work demonstrates the feasibility of the new preparation approach to obtain membranes which may be advantageous due to the fact that the studied Pebax® code is only soluble in an alcohol (1-propanol/1-butanol) mixture. This suggests higher chemical stability of the obtained membranes when exposed to moisture since typical Pebax® 1657 membranes are obtained from water/ethanol polymer solutions.

Moreover, to study the CO<sub>2</sub> and N<sub>2</sub> permeance, as well as the CO<sub>2</sub>/N<sub>2</sub> selectivity dependence of temperature, gas permeation tests were also carried out at 25 and 50 °C and the same pressure conditions (3 bar) with the membrane which offered the best separation properties, 0.5 wt%<sub>4</sub> as demonstrated in Fig. 8. As observed in Fig. S10 of the SI, whereas the CO<sub>2</sub> and N<sub>2</sub> permeance increased almost linearly with temperature, the CO<sub>2</sub>/N<sub>2</sub> selectivity decreased, due to the thermal activation process which favored N<sub>2</sub> over CO<sub>2</sub> transport. This behavior was studied more in depth applying an Arrhenius modified model to the data of CO<sub>2</sub> and N<sub>2</sub> permeance and temperature (see Eq. S1 and Fig. S11) [5,37]. Based on this model, the activation energy (E<sub>p</sub>) of the Pebax® 3533 supported membranes associated to the CO<sub>2</sub> and N<sub>2</sub> permeations were 14.2 kJ mol<sup>-1</sup> and 29.6 kJ mol<sup>-1</sup>, respectively, close to the values found in the literature for other Pebax®-type membranes (in the ranges of 13.3–18.2 kJ mol<sup>-1</sup> for CO<sub>2</sub> and 27.2–32.0 kJ mol<sup>-1</sup> for N<sub>2</sub>) (see Table 2). It must be noted that the activation energies of both composite and self-supported membranes are comparable. This suggests that the Pebax® selective layer is the main responsible of the final separation properties in a composite membrane. Additionally, the higher activation energy of N<sub>2</sub> with respect to that of CO<sub>2</sub> justifies the reduction of the CO<sub>2</sub>/N<sub>2</sub> selectivity as a function of temperature, as shown in Fig. S10b of the SI [38].

**Table 3**

Comparison of experimental and RSM (resistance in series model) calculated values for permeance and resistance of TFC membranes prepared with the 0.5 wt% casting solution.

Membrane	Permeance (GPU)		Total resistance (GPU <sup>-1</sup> m <sup>-2</sup> )		Pebax® resistance (GPU <sup>-1</sup> m <sup>-2</sup> )	
	Experimental	RSM	Experimental	RSM	RSM	Contribution to total resistance (%)
0.5 wt%_3	101 ± 3	168	46.7	28.1	8.6	31
0.5 wt%_4	127 ± 10	137	37.1	34.5	15.0	44
0.5 wt%_5	105 ± 6	115	44.9	40.9	21.4	52
0.5 wt%_6	64 ± 3	100	73.7	47.4	27.9	59

### 3.3. Membrane calculations: resistance in series model (RSM)

The flow rate of a gas through a membrane can be expressed as a function of a resistance to flow [42]. According to this statement, gas transport through a layered membrane can be described as an analogy to the electric flow in the serial connection of conductors. In this sense, each layer provides a resistance to the flow proportional to the thickness and inversely proportional to its permeability and surface area (see Eq. S2). Based on this model, the total resistance and permeance of a composite membrane can be estimated by Eqs. S3 and S6, respectively, using permeability values of 96800 and 220 Barrer for the PSF porous support and the Pebax® 3533 polymer, respectively. The theoretical performance of the membranes fabricated with the 0.5 wt% casting solution was estimated using the equations above mentioned and the results can be found in Table 3 and Fig. S13. As seen in this figure, greater permeance values should be obtained as calculated by the resistance-in-series model (i.e. 162 GPU vs. 127 GPU and 111 GPU vs. 105 GPU for the membranes composed of 4 and 5 Pebax® layers, respectively). As mentioned in previous sections, filling of large support pores could be the cause of such reduction since theoretical calculations assume that the Pebax® solution did not penetrate into the support porosity. Furthermore, the deviation found with the membrane composed of 3 Pebax® layers could be due to the presence of defects in the selective layer, which hinder the selective diffusion of CO<sub>2</sub> molecules. For this reason, additional layers are needed to obtain a better performance, as experimentally determined. Additionally, the contribution of Pebax® layers to the overall resistance of the composite membrane has been calculated. As seen in Table 3, the experimental Pebax® layer resistance of membranes composed of 4 and 5 layers was the closest to those estimated with the resistance-in-series model. Finally, the contribution of Pebax® to the total resistance increases from 31% to 59% when the number of Pebax® went from 3 to 6 (see Table 3), in line with the achievement of the optimum separation conditions of the composite membranes.

## 4. Conclusions

A phase inversion method has been developed in this work for the preparation of Pebax® 3533 supported membranes. The method consisting of the deposition of various thin layers of Pebax® on top of polysulfone porous supports was optimized and the influence of the casting solution concentration, as well as the number of polymer layers was studied. The polymer concentration in the casting solution altered its viscosity with the consequent impact on the gas separation performance. Moreover, the application of additional polymer layers allowed to repair the micro-defects improving the membrane selectivity. The characterization of the chemical structure of the membranes by FTIR showed the correct deposition of the Pebax® layers on top of the PSF supports for the membranes prepared with the 1.5, 1.0 and 0.5 wt% casting solution concentration. The thermal stability of the membranes was confirmed by TGA. Regarding the CO<sub>2</sub>/N<sub>2</sub> separation performance, the dilution of the casting solution concentration together with the appropriate number of Pebax® layers allowed to increase the CO<sub>2</sub> permeance. The best performance was obtained with the membranes prepared with the 0.5 wt% casting solution after the deposition of 4 layers,

reaching a CO<sub>2</sub> permeance of 127 ± 10 GPU and a CO<sub>2</sub>/N<sub>2</sub> selectivity of 21.4. The implementation of the phase inversion method for the coating of dense selective layers was also validated by testing the gas separation performance of supported membranes prepared by dip-coating. Additionally, the activation energy values for permeance (14.2 kJ mol<sup>-1</sup> for CO<sub>2</sub> and 29.6 kJ mol<sup>-1</sup> for N<sub>2</sub>) revealed the analogy of these supported membranes with dense membranes prepared with other codes of Pebax®.

### CRediT authorship contribution statement

**Lidia Martínez-Izquierdo:** Conceptualization, Methodology, Validation, Formal analysis, Investigation, Writing - original draft, Review, Visualization. **Magdalena Malankowska:** Conceptualization, Verification, Writing - original draft, Review, Supervision. **Carlos Téllez:** Conceptualization, Verification, Writing - original draft, Review, Funding acquisition, supervision. **Joaquín Coronas:** Conceptualization, Verification, Writing - original draft, review, Funding acquisition, Supervision.

### Declaration of Competing Interest

The authors declare that they have no known competing financial interests or personal relationships that could have appeared to influence the work reported in this paper.

### Acknowledgments

Financial support from the Spanish Research Projects MAT2016-77290-R (MINECO/AEI, FEDER/UE), PID2019-104009RB-I00/AEI/10.13039/501100011033 (Agencia Estatal de Investigación, Spain) and T43-20R (the Aragón Government and ESF) is gratefully acknowledged. L. Martínez-Izquierdo also thanks the Aragón Government (DGA) for her PhD grant. All microscopy work was done in the Laboratorio de Microscopías Avanzadas at the Instituto de Nanociencia de Aragón (LMA-INA).

### Appendix A. Supporting information

Supplementary data associated with this article can be found in the online version at [doi:10.1016/j.jece.2021.105624](https://doi.org/10.1016/j.jece.2021.105624).

### References

- [1] M. Kárászová, B. Zach, Z. Petrusová, V. Červenka, M. Bobák, M. Šyc, P. Izák, Post-combustion carbon capture by membrane separation, review, Sep. Purif. Technol. 238 (2020), 116448, <https://doi.org/10.1016/j.seppur.2019.116448>.
- [2] J. Sánchez-Láinez, A. Pardillos-Ruiz, M. Carta, R. Malpass-Evans, N.B. McKeown, C. Téllez, J. Coronas, Polymer engineering by blending PIM-1 and 6FDA-DAM for ZIF-8 containing mixed matrix membranes applied to CO<sub>2</sub> separations, Sep. Purif. Technol. 224 (2019) 456–462, <https://doi.org/10.1016/j.seppur.2019.05.035>.
- [3] C. Chao, Y. Deng, R. Dewil, J. Baeyens, X. Fan, Post-combustion carbon capture, Renew. Sustain. Energy Rev. 138 (2021), 110490, <https://doi.org/10.1016/j.rser.2020.110490>.
- [4] J. Sánchez-Láinez, M. Ballester-Catalán, E. Javierre-Ortín, C. Téllez, J. Coronas, Pebax® 1041 supported membranes with carbon nanotubes prepared: via phase inversion for CO<sub>2</sub>/N<sub>2</sub> separation, Dalton Trans. 49 (2020) 2905–2913, <https://doi.org/10.1039/c9dt04424h>.



- [5] L. Martínez-Izquierdo, M. Malankowska, J. Sánchez-Laínez, C. Téllez, J. Coronas, Poly(ether-block-amide) copolymer membrane for CO<sub>2</sub>/N<sub>2</sub> separation: The influence of the casting solution concentration on its morphology, thermal properties and gas separation performance, *R. Soc. Open Sci.* 6 (2019), 190866, <https://doi.org/10.1098/rsos.190866>.
- [6] S.R. Reijerkerk, M.H. Knoef, K. Nijmeijer, M. Wessling, Poly(ethylene glycol) and poly(dimethyl siloxane): combining their advantages into efficient CO<sub>2</sub> gas separation membranes, *J. Memb. Sci.* 352 (2010) 126–135, <https://doi.org/10.1016/j.memsci.2010.02.008>.
- [7] F. Pazani, A. Aroujalian, Enhanced CO<sub>2</sub>-selective behavior of Pebax-1657: a comparative study between the influence of graphene-based fillers, *Polym. Test.* 81 (2020), 106264, <https://doi.org/10.1016/j.polymertesting.2019.106264>.
- [8] Y. Zheng, Y. Wu, B. Zhang, Z. Wang, Preparation and characterization of CO<sub>2</sub>-selective Pebax/NaY mixed matrix membranes, *J. Appl. Polym. Sci.* 137 (2020) 48398, <https://doi.org/10.1002/app.48398>.
- [9] J. Wang, W. Fang, J. Luo, M. Gao, Y. Wan, S. Zhang, X. Zhang, A.-H.A. Park, Selective separation of CO<sub>2</sub> using novel mixed matrix membranes based on Pebax and liquid-like nanoparticle organic hybrid materials, *J. Memb. Sci.* 584 (2019) 79–88, <https://doi.org/10.1016/j.memsci.2019.04.079>.
- [10] P. Bernardo, G. Clarizia, Enhancing gas permeation properties of Pebax® 1657 membranes via polysorbate nonionic surfactants doping, *Polymers* 12 (2020) 253, <https://doi.org/10.3390/polym12020253>.
- [11] X. Ren, J. Ren, H. Li, S. Feng, M. Deng, Poly (amide-6-b-ethylene oxide) multilayer composite membrane for carbon dioxide separation, *Int. J. Greenh. Gas Control.* 8 (2012) 111–120, <https://doi.org/10.1016/j.ijggc.2012.01.017>.
- [12] T.C. Merkel, H. Lin, X. Wei, R. Baker, Power plant post-combustion carbon dioxide capture: an opportunity for membranes, *J. Membr. Sci.* 359 (2010) 126–139, <https://doi.org/10.1016/j.memsci.2009.10.041>.
- [13] L.M. Robeson, The upper bound revisited, *J. Memb. Sci.* 320 (2008) 390–400, <https://doi.org/10.1016/j.memsci.2008.04.030>.
- [14] J. Benito, J. Sánchez-Laínez, B. Zornoza, S. Martín, M. Carta, R. Malpass-Evans, C. Téllez, N.B. Mckeown, J. Coronas, I. Gascón, Ultrathin composite polymeric membranes for CO<sub>2</sub>/N<sub>2</sub> separation with minimum thickness and high CO<sub>2</sub> permeance, *ChemSusChem* 10 (2017) 4014–4017, <https://doi.org/10.1002/cssc.201701139>.
- [15] Y. Wu, D. Zhao, J. Ren, Y. Qiu, M. Deng, A novel Pebax-C<sub>60</sub>(OH)<sub>24</sub>/PAN thin film composite membrane for carbon dioxide capture, *Sep. Purif. Technol.* 215 (2019) 480–489, <https://doi.org/10.1016/j.seppur.2018.12.073>.
- [16] M.M. Rahman, C. Abetz, S. Shishatskiy, J. Martin, A.J. Muñller, V. Abetz, CO<sub>2</sub> Selective polyactive membrane: thermal transitions and gas permeance as a function of thickness, *Appl. Mater. Interfaces* 10 (2018) 26733–26744, <https://doi.org/10.1021/acsami.8b09259>.
- [17] J.M.P. Scofield, P.A. Gurr, J. Kim, Q. Fu, A. Halim, S.E. Kentish, G.G. Qiao, High-performance thin film composite membranes with well-defined poly (dimethylsiloxane)-b-poly(ethylene glycol) copolymer additives for CO<sub>2</sub> separation, *J. Polym. Sci. Part A Polym. Chem.* 53 (2015) 1500–1511, <https://doi.org/10.1002/pola.27628>.
- [18] J.M.P. Scofield, P.A. Gurr, J. Kim, Q. Fu, S.E. Kentish, G.G. Qiao, Blends of fluorinated additives with highly selective thin-film composite membranes to increase CO<sub>2</sub> permeability for CO<sub>2</sub>/N<sub>2</sub> gas separation applications, *Ind. Eng. Chem. Res.* 55 (2016) 8364–8372, <https://doi.org/10.1021/acs.iecr.6b02167>.
- [19] J. Sánchez-Laínez, L. Paseta, M. Navarro, B. Zornoza, C. Téllez, J. Coronas, Ultraporous thin film ZIF-8/polyamide membrane for H<sub>2</sub>/CO<sub>2</sub> separation at high temperature without using sweep gas, *Adv. Mater. Interfaces* 5 (2018), 1800647, <https://doi.org/10.1002/admi.201800647>.
- [20] D. Zhao, Y. Wu, J. Ren, H. Li, Y. Qiu, M. Deng, Improved CO<sub>2</sub> separation performance of composite membrane with the aids of low-temperature plasma treatment, *J. Membr. Sci.* 570–571 (2019) 184–193, <https://doi.org/10.1016/j.memsci.2018.10.051>.
- [21] J.H. Kim, Y. Ha, Y.M. Lee, Gas permeation of poly(amide-6-b-ethylene oxide) copolymer, *J. Membr. Sci.* (2001).
- [22] T. Jauzein, M.A. Huneault, M.C. Heuzey, Crystallinity and mechanical properties of polylactide/ether-amide copolymer blends, *J. Appl. Polym. Sci.* 134 (2017) 44677, <https://doi.org/10.1002/app.44677>.
- [23] D.M. Devine, L.M. Geever, C.L. Higginbotham, Drug release from a N-vinylpyrrolidone/acrylic acid lubricious hydrophilic coating, *J. Mater. Sci.* 40 (2005) 3429–3436, <https://doi.org/10.1007/s10853-005-0416-2>.
- [24] L. Paseta, M. Navarro, J. Coronas, C. Téllez, Greener processes in the preparation of thin film nanocomposite membranes with diverse metal-organic frameworks for organic solvent nanofiltration, *J. Ind. Eng. Chem.* 77 (2019) 344–354, <https://doi.org/10.1016/j.jiec.2019.04.057>.
- [25] T. Tavangar, Farzin, Z. Ashtiani, M. Karimi, Morphological and performance evaluation of highly sulfonated polyethersulfone/polyethersulfone membrane for oil/water separation, *J. Polym. Res.* 27 (2020) 252, <https://doi.org/10.1007/s10965-020-02202-5>.
- [26] S.S. Swain, L. Unnikrishnan, S. Mohanty, S.K. Nayak, Gas permeation and selectivity characteristics of PSf based nanocomposite membranes, *Polymer* 180 (2019), 121692, <https://doi.org/10.1016/j.polymer.2019.121692>.
- [27] I. Ullah Khan, M. Hafiz, D. Othman, A. Jilani, A.F. Ismail, H. Hashim, J. Jaafar, A. K. Zulhairun, M.A. Rahman, G.U. Rehman, ZIF-8 based polysulfone hollow fiber membranes for natural gas purification, *Polym. Test.* 84 (2020), 106415, <https://doi.org/10.1016/j.polymertesting.2020.106415>.
- [28] M. Elyasi Kojabad, M. Momeni, A.A. Babaluo, M.J. Vaezi, PEBA/PSf multilayer composite membranes for CO<sub>2</sub> separation: influence of dip coating parameters, *Chem. Eng. Technol.* 43 (2020) 1451–1460, <https://doi.org/10.1002/ceat.201900262>.
- [29] H. Sanaeepur, S. Mashhadikhan, G. Mardassi, A. Ebadi Amooghin, B. Van der Bruggen, A. Moghadassi, Aminosilane cross-linked poly ether-block-amide PEBAX 2533: characterization and CO<sub>2</sub> separation properties, *Korean J. Chem. Eng.* 36 (2019) 1339–1349, <https://doi.org/10.1007/s11814-019-0323-x>.
- [30] L. Eykens, K. De Sitter, L. Stoops, C. Dotremont, L. Pinoy, B. Van Der Bruggen, Development of polyethersulfone phase-inversion membranes for membrane distillation using oleophobic coatings, *J. Appl. Polym. Sci.* 134 (2017) 45516, <https://doi.org/10.1002/app.45516>.
- [31] L. Sugu, Z.A. Jawad, Formation of low acetyl content cellulose acetate membrane for CO<sub>2</sub>/N<sub>2</sub> separation, *J. Phys. Sci.* 30 (2019) 111–125, <https://doi.org/10.21315/jps2019.30.1.9>.
- [32] R.A. Roslan, W.J. Lau, A.K. Zulhairun, P.S. Goh, A.F. Ismail, Improving CO<sub>2</sub>/CH<sub>4</sub> and O<sub>2</sub>/N<sub>2</sub> separation by using surface-modified polysulfone hollow fiber membranes, *J. Polym. Res.* 27 (2020) 1–14, <https://doi.org/10.1007/s10965-020-02104-6>.
- [33] J. Sánchez-Laínez, B. Zornoza, C. Téllez, J. Coronas, Asymmetric polybenzimidazole membranes with thin selective skin layer containing ZIF-8 for H<sub>2</sub>/CO<sub>2</sub> separation at pre-combustion capture conditions, *J. Memb. Sci.* 563 (2018) 427–434, <https://doi.org/10.1016/j.memsci.2018.06.009>.
- [34] S.A. Mohammed, A.M. Nasir, F. Aziz, G. Kumar, W. Sallehuddin, J. Jaafar, W. J. Lau, N. Yusof, W.N.W. Salleh, A.F. Ismail, CO<sub>2</sub>/N<sub>2</sub> selectivity enhancement of PEBAX MH 1657/aminated partially reduced graphene oxide mixed matrix composite membrane, *Sep. Purif. Technol.* 223 (2019) 142–153, <https://doi.org/10.1016/j.seppur.2019.04.061>.
- [35] M. Elyasi Kojabad, M. Momeni, A.A. Babaluo, M.J. Vaezi, PEBA/PSf multilayer composite membranes for CO<sub>2</sub> separation: influence of dip coating parameters, *Chem. Eng. Technol.* 43 (2020) 1451–1460, <https://doi.org/10.1002/ceat.201900262>.
- [36] Q. Fu, A. Halim, J. Kim, J.M.P. Scofield, P.A. Gurr, S.E. Kentish, G.G. Qiao, Highly permeable membrane materials for CO<sub>2</sub> capture, *J. Mater. Chem. A.* 1 (2013) 13769–13778, <https://doi.org/10.1039/c3ta13066e>.
- [37] S. Feng, J. Ren, D. Zhao, H. Li, K. Hua, X. Li, M. Deng, Effect of poly(ethylene glycol) molecular weight on CO<sub>2</sub>/N<sub>2</sub> separation performance of poly(amide-12-b-ethylene oxide)/poly(ethylene glycol) blend membranes, *J. Energy Chem.* 28 (2019) 39–45, <https://doi.org/10.1016/j.jechem.2017.10.014>.
- [38] T. Zhu, X. Yang, Y. Zheng, X. He, F. Chen, J. Luo, Preparation of poly(ether-block-amide)/poly(amide-co-poly(propylene glycol)) random copolymer blend membranes for CO<sub>2</sub>/N<sub>2</sub> separation, *Polym. Eng. Sci.* 59 (2019) E14–E23, <https://doi.org/10.1002/pen.24828>.
- [39] A. Tena, S. Shishatskiy, V. Filiz, Poly(ether-amide) vs. poly(ether-imide) copolymers for post-combustion membrane separation processes, *RSC Adv.* 5 (2015) 22310–22318, <https://doi.org/10.1039/c5ra01328c>.
- [40] M.M. Rahman, V. Filiz, S. Shishatskiy, C. Abetz, S. Neumann, S. Bolmer, M. Khan, V. Abetz, PEBAX® with PEG functionalized POSS as nanocomposite membranes for CO<sub>2</sub> separation, *J. Membr. Sci.* 437 (2013) 286–297, <https://doi.org/10.1016/j.memsci.2013.03.001>.
- [41] E. Tocci, A. Gugliuzza, L. De Lorenzo, M. Macchione, G. De Luca, E. Drioli, Transport properties of a co-poly(amide-12-b-ethylene oxide) membrane: a comparative study between experimental and molecular modelling results, *J. Membr. Sci.* 323 (2008) 316–327, <https://doi.org/10.1016/j.memsci.2008.06.031>.
- [42] J. Lillepär, S. Breitenkamp, S. Shishatskiy, J. Pohlmann, J. Wind, C. Scholles, T. Brinkmann, Characteristics of gas permeation behaviour in multilayer thin film composite membranes for CO<sub>2</sub> separation, *Membranes* 9 (2019) 22, <https://doi.org/10.3390/membranes9020022>.